Published in final edited form as:
Eur J Pharm Biopharm. 2014 April ; 86(3): 514–523. doi:10.1016/j.ejpb.2013.12.009.

The development of orally administrable gemcitabine prodrugs with D-enantiomer amino acids: Enhanced membrane permeability and enzymatic stability

Yasuhiro Tsume[a], **Tuba Incecayir**[b], **Xueqin Song**[c], **John M. Hilfinger**[d], and **Gordon L. Amidon**[a]

[a]Department of Pharmaceutical Science, University of Michigan, Ann Arbor, MI, USA

[b]Department of Pharmaceutical Technology, Gazi University, Etiler-Ankara, Turkey

[c]Hospira, Inc., Lake Forest, IL, USA

[d]TSRL, Inc., Ann Arbor, MI, USA

Abstract

Gemcitabine prodrugs with D- and L-configuration amino acids were synthesized and their chemical stability in buffers, resistance to glycosidic bond metabolism, enzymatic activation, permeability in Caco-2 cells and mouse intestinal membrane, anti-proliferation activity in cancer cell were determined and compared to that of parent drug, gemcitabine. Prodrugs containing D-configuration amino acids were enzymatically more stable than ones with L-configuration amino acids. The activation of all gemcitabine prodrugs was 1.3–17.6-fold faster in cancer cell homogenate than their hydrolysis in buffer, suggesting enzymatic action. The enzymatic activation of amino acid monoester prodrugs containing D-configuration amino acids in cell homogenates was 2.2–10.9-fold slower than one of amino acid monoester prodrugs with L-configuration amino acids. All prodrugs exhibited enhanced resistance to glycosidic bond metabolism by thymidine phosphorylase compared to parent gemcitabine. Gemcitabine prodrugs showed superior the effective permeability in mouse jejunum to gemcitabine. More importantly, the high plasma concentration of D-amino acid gemcitabine prodrugs was observed more than one of L-amino acid gem-citabine prodrugs. In general, the 5′-mono-amino acid monoester gemcitabine prodrugs exhibited higher permeability and uptake than their parent drug, gemcitabine. Cell proliferation assays in AsPC-1 pancreatic ductal cell line indicated that gemcitabine prodrugs were more potent than their parent drug, gemcitabine. The transport and enzymatic profiles of 5′-D-valyl-gemcitabine and 5′-D-phenylalanyl-gem-citabine suggest their potential for increased oral uptake and delayed enzymatic bioconversion as well as enhanced uptake and cytotoxic activity in cancer cells, would facilitate the development of oral dosage form for anti-cancer agents and, hence, improve the quality of life for the cancer patients.

*Corresponding author. College of Pharmacy, The University of Michigan, 428 Church Street, Ann Arbor, MI 48109-1065, USA. Tel.: +1 734 764 2440; fax: +1 734 763 6423. glamidon@umich.edu (G.L. Amidon).

Keywords

Monoester gemcitabine prodrugs; Mouse *in situ* perfusion; Unnatural form; Amino acid; Stability; Permeability

1. Introduction

The anti-cancer agent 2,2′-difluoro-2′-deoxyuridine or Gemzar® (gemcitabine), one of the nucleoside analogs, has been used to treat pancreatic and non-small-cell lung cancers as the first-line therapy [1,2]. However, the adverse effects associated with chemo-therapeutics are still unresolved and many efforts have been made to minimize side-effects and maximize therapeutic efficacy. Prodrug strategies have been utilized to overcome undesirable physicochemical properties of the drug, to improve oral bioavail-ability. A majority of the efforts have focused on anti-viral and anti-cancer drugs to develop oral alternatives. Amino acid ester prodrugs of poorly permeable anti-cancer and anti-viral drugs have been designed for targeted delivery *via* specific transporters to improve their oral bioavailability and metabolic disposition [2–11].

Amino acid ester anti-cancer prodrugs have been synthesized and tested for potential improvement of oral drug delivery [5,10–15]. It has been reported that amino acid ester prodrugs are recognized as substrates for intake transporters such as PEPT1, PEPT2, and $ATB^{0,+}$, and this carrier-mediated mechanism improves their oral bioavailability [10,13,16–21]. PEPT1 is predominantly expressed in the small intestine and can transport dipeptides, trip-eptides, amino acid monoester prodrugs and β-lactam antibiotics [10,11,16,22–28]. PEPT1 has broad substrate specificity and recognizes D-enantiomers of amino acid as a substrate even though PEPT1 is stereoselective and exhibits greater affinity for L-enantiomers of amino acids than D-enantiomers [10,29,30]. Amino acid ester prodrugs may facilitate enhanced delivery to pancreatic cancer cells such as AsPC-1 due to the high expression of oligopeptide transporters [31].

The mechanism of action for anti-cancer nucleoside analogs such as 5-Fluorouracil (5-FU), floxuridine, and gemcitabine is well investigated and understood [32–35]. Most of anti-cancer drugs including nucleoside analogs are intravenously administered due to their low oral bioavailability and stability issues [36,37]. Moreover, nucleoside analogs are enzymatically converted to pyrimidine structure in many tissues including the liver [37,38]. As a consequence, higher doses of chemotherapeutic agents are required to assure clinical efficacy, leading to greater toxicity. Oral anti-cancer therapy obviously improves the quality of life for cancer patients compared to intravenous therapy because of its convenience and, eventually, the reduction in insurance costs [39]. Improving the chemical and enzymatic stabilities and membrane permeability of gemcitabine may enhance its therapeutic efficacy at low doses and obviate toxicity concerns with orally administrable chemotherapeutic drugs.

In this report, we describe the stability and permeability of (D-/ L-)amino acid monoester prodrugs of gemcitabine, as well as their antiproliferative activity. Uptake studies were conducted with Caco-2 and AsPC-1 cells and permeability studies were conducted with

Caco-2 cell monolayer and *in situ* mouse jejunal perfusion. Furthermore, the feasibility of developing orally administrable chemotherapeutic agents was assessed by measuring the drug concentration and drug species in plasma after the perfusion study. The chemical stability at physiological pH and the enzymatic activation of the prodrugs in Caco-2, and AsPC-1 cell homogenates as well as thymidine phosphorylase were also evaluated to determine the effects of the amino acid configuration on enzyme-mediated activation. The antiproliferative action of amino acid gemcitabine prodrugs and their parent drug, gemcitabine, was explored using pancreatic ductal cancer cell, AsPC-1.

2. Materials and methods

2.1. Materials

Gemcitabine was extracted from the lyophilized powder (Gem-zar) supplied by Eli Lilly Pharmaceuticals (Indianapolis, IN). The tert-butyloxycarbonyl (Boc) protected amino acids Boc-L-valine, Boc- D-valine, Boc-L-phenylalanine, and Boc- D-phenylalanine were obtained from Chem-Impex (Wood Dale, IL). High-performance liquid chromatography (HPLC) grade acetonitrile was obtained from Fisher Scientific (St. Louis, MO). N,N-dicyclohexylcarbodiimide (DCC), N,N-dimethylaminopyridine (DMAP), trifluoroacetic acid (TFA), and all other reagents and solvents were purchased from Al-drich Chemical Co. (Milwaukee, WI). Cell culture reagents were obtained from Invitrogen (Carlsbad, CA) and cell culture supplies were obtained from Corning (Corning, NY) and Falcon (Lincoln Park, NJ). All chemicals were of either analytical or HPLC grade.

2.2. Gemcitabine prodrug synthesis

The synthesis and characterization of 5′-mono-amino acid ester prodrugs of gemcitabine have been reported previously [5]. Briefly, Boc-protected amino acid, Boc-L-valine, Boc-D-valine, Boc-L-phen-ylalanine, or Boc- D-phenylalanine, (1.1 mmol), DCC (1.1 mmol), and DMAP (0.1 mmol) were allowed to react with gemcitabine (1 mmol) in 7 mL of dry DMF for 24 h. The reaction progress was monitored by thin layer chromatography (TLC) (ethyl acetate). The reaction mixture was filtered and dichloromethane (DCM) was removed under vacuum at 40 °C. The residue was extracted with ethyl acetate (30 mL) and washed with water (2 × 20 mL), and saturated NaCl (20 mL). The organic layer was dried over $MgSO_4$ and concentrated under vacuum. The reaction yielded a mixture of gemcitabine Boc-protected prodrugs. The three spots observed on TLC were separated and purified using column chromatography (dichloromethane/methanol, 20:1). Fractions from each spot (the first spot: 5′-monoester gemcitabine prodrug, the second spot: 3′-monoester gemcitabine prodrug, and the third spot: 3′,5′-diester gemcitabine prodrug) were concentrated under vacuum separately. The Boc group was cleaved by treating the residues with 5 mL TFA:DCM (1:1). After 4 h, the solvent was removed and the residues were reconstituted with water and lyophilized. The TFA salts of amino acid prodrugs of gemcitabine were obtained as white fluffy solids. The yield of 5′-mono-amino acid gemcitabine prodrug was 12–20%. HPLC was used to evaluate the prodrug purity. Prodrugs were between 90–99% pure. These prodrugs were easily separated from parent drug by HPLC. Electrospray ionization mass spectra (ESI-MS) were obtained on a Micromass LCT ESI-MS. The observed molecular weights of all prodrugs were found to be consistent with that required

by their structure. The structural identity of the prodrugs was then confirmed using proton nuclear magnetic resonance spectra (^{1}H NMR). ^{1}H NMR spectra were obtained on a 300 MHz Bruker DPX-300 NMR spectrometer.

2.3. Cell culture

AsPC-1 cells (passages 25–38) from American type Culture Collection (Rockville, MD) were routinely maintained in RPMI-1640 containing 10% fetal bovine serum. Caco-2 cells (passages 28–31) from American type Culture Collection (Rockville, MD) were routinely maintained in DMEM containing 10% fetal bovine serum. Cells were grown at 37 °C at 5% CO_2 and 90% relative humidity in antibiotic-free media to avoid the possible transport interference by antibiotics.

2.4. Hydrolysis studies

2.4.1. Enzymatic stability—Confluent Caco-2 and AsPC-1cells were rinsed twice with phosphate buffered saline (PBS). The cells were lysed with phosphate buffer (pH 7.4) by ultrasonication (Micro ultrasonic cell disrupter Model KT40, Kontes, Vineland, NJ, USA), and pelleted by centrifugation for 5 min at 1000g. The protein amount was quantified with the Bio-Rad (Hercules, CA, USA) DC Protein Assay using bovine serum albumin as a standard. The amount of protein was adjusted to 500 μg/mL and hydrolysis reactions were carried out in 96-well plates (Corning, NY, USA). Caco-2 and AsPC-1 cell suspensions (250 μL) were placed in triplicate wells, the reactions were started with the addition of substrate, and cells were incubated at 37 °C for 120 min. At the desired time point, sample aliquots (35 μL) were removed and added to acetonitrile (ACN, 150 μL) with 0.1% TFA. The mixtures were filtered with a 0.45 μm filter membrane at 1000*g* for 10 min at 4 °C. The filtrate was then analyzed via reverse-phase HPLC.

2.4.2. Chemical stability—The nonenzymatic hydrolysis of the prodrugs was determined as described above, except that each well contained pH 7.4 phosphate buffers (10 mmol/L) instead of cell homogenate. Also, the chemical stability of the prodrugs was determined in simulated gastric fluid (SGF) pH 1.2 and simulated intestinal fluid (SIF) pH 6.8.

2.4.3. Microsomal stability—The assay was performed in triplicate containing substrates, 500 μg/mL of microsomal proteins diluted in PBS (pH 7.4) and 16.7 mg/mL of β-nicotinamide-adenine dinucleotide phosphate (NADPH). After applying NADPH solution into the microsomal suspension (250 μL) containing substrates, the sample was immediately taken as $t = 0$. The sample mixtures were incubated at 37 °C for 120 min. At the desired time point, sample aliquots (30 μL) were removed and added to acetonitrile (ACN, 150 μL) with 0.1% TFA. The mixtures were filtered with a 0.45 μm filter membrane at 1000*g* for 10 min at 4 °C. The filtrate was then analyzed via reverse-phase HPLC.

2.5. Uptake studies

Caco-2 and AsPC-1 cells were grown on a 6-well plate for 18 and 6 days, respectively. Wells were rinsed with MES (pH 6.0) buffer twice. Fresh MES buffer was reapplied to each well and incubated at 37 °C for 15 min. Each drug was individually tested from freshly prepared solutions in MES buffer (0.1 mM, total 0.3 mL) with both the presence and the

absence of 10 mM glycyl-proline (Gly-Pro). Additionally, uptake studies with the lower drug concentration, 0.05 mM, in AsPC-1 cells were carried out to determine the dose linearity. The solution was placed in each well and incubated at 37 °C for 60 min. Drug solution was removed and 3 mL of ice-cold PBS was immediately placed in each well. Each well was rinsed with 3 mL of cold-PBS twice and 0.5 mL of methanol:H_2O (1:1) containing 0.1% TFA was placed in each well. The cell suspension was collected and transferred to a new tube. Those tubes were spun at 1000*g* at 4 °C for 5 min. The supernatant was mixed with an equal amount of water for HPLC analysis. The cell pullets were used to determine the protein amount with the Bio-Rad (Hercules, CA, USA) DC Protein Assay using bovine serum albumin as a standard.

2.6. Caco-2 cell monolayer permeability studies

Caco-2 cell monolayers were grown on collagen-coated polytet-rafluoroethylene membrane for 21–24 days. Transepithelial electrical resistance (TEER) was monitored and values of 550–600 Ω cm^2 (total growth area was 1.12 cm^2) were used in the study. Apical and basolateral sides of transwell inserts were washed with MES (pH 6.0) and HEPES (pH 7.4), respectively. Fresh MES and HEPES buffers were reapplied to transwell inserts and incubated at 37 °C for 15 min. Each drug was individually tested from freshly prepared solutions in MES buffer (0.1 mM, total 0.5 mL) with both the presence and the absence of 10 mM Gly-Pro. The solution was placed in the donor chamber, while the receiver chamber was filled with HEPES buffer (total 1.5 mL). Sampling from the receiver chamber was conducted up to a period of 2 h at time intervals of 15, 30, 45, 60, 75, 90, and 120 min, at 37 °C and replaced with an equal volume of fresh HEPES buffer to maintain sink conditions in the receiver chamber. All samples were immediately acidified with 0.1% TFA and analyzed by HPLC.

2.7. Solution for single-pass intestinal perfusion

The perfusion buffer (pH 6.0) consisted of 145 mM NaCl, 0.5 mM $MgCl_2$, 1 NaH_2PO_4, 1 mM $CaCl_2$, 3 mM KCl, 5 mM glucose, and 5 mM MES. The pH of the buffer was adjusted to pH 6.0. This perfusion buffer also contained phenol-red (14 μM) as a non-absorbable marker for water flux measurements.

2.8. Single-pass intestinal perfusion studies in mice

All animal experiments were conducted using protocols approved by the University of Michigan Committee of Use and Care of Animals (UCUCA). Female BALB/c mice (Charles River, IN) weighing 20–25 g were used for all perfusion studies. Prior to each experiment, mice were fasted overnight with free access to water.

The procedure for the *in situ* single-pass intestinal perfusion is previously reported [40]. Briefly, mice were anesthetized with an i.m. injection of ketamine-xylazine mixture (ketamine: 80–120 mg/kg, xylazine: 5–10 mg/kg) and placed on a heated pad maintained at 37 °C. The abdomen was opened by a midline incision and a jejunal segment (approximately 10 cm) was carefully exposed to cannulate both ends with flexible polyvinyl chloride (PVC) tubing (2.06 mm i.d., Fisher Scientific Inc., Pittsburgh, PA, USA). All

solutions were incubated in a 37 °C water-bath. The isolated segment was rinsed with blank perfusion buffer to clean out any residual debris.

At the start of the study, the test compound (100 μM) in perfusion buffer (pH 6.0) including phenol red was perfused through the intestinal segment (Watson-Marlow Pumps 323S, Watson-Marlow Bredel Inc., Wilimington, MA), at the flow rate of 0.08 mL/min. The perfusion buffer was perfused for 30 min to assure steady-state and samples were taken every 10 min for 90 min. At the end of perfusion, blood samples were collected by cardiac puncture. Blood samples with heparin were centrifuged at 1000*g* for 10 min at 4 °C to collect plasma samples for LC–MS analysis. Following the termination of the experiment, the length of each perfused intestinal segment was measured.

2.9. Cell proliferation assays

Cell proliferation studies were conducted with AsPC-1 cells. The cells were seeded into 96-well plates at 125,000 cells per well and allowed to attach/grow for 24 h before drug solutions were added. The culture medium (RPMI-1640 + 10% fetal bovine serum) was removed and the cells were gently washed once with sterile pH 6.0 uptake buffer. Gemcitabine and gemcitabine prodrugs were 2-fold serially diluted in pH 6.0 uptake buffer from 5 to 0.078 mmol/L. Buffer alone was used as a 100% viability control. The wash buffer was removed and 30 μL drug solution per well was added and incubated at 37 °C for 2 h in the cell incubator. After this time, the drug solutions were removed and the cells were again gently washed twice with sterile uptake buffer. The culture medium was then added to each well after washing. The cells were allowed to recover for 24 h before evaluating cell viability via 2,3-bis[2-methoxy-4-nitro-5-sulfophenyl]-2H-tetrazolium-5-carboxanilide inner salt (XTT) assays. A mixture (30 μL) containing XTT (1 mg/ mL) in sterile RPMI-1640 without phenol red and phenazine methosulfate (N-methyldibenzopyrazine methyl sulfate in sterile PBS, 0.383 mg/mL) reagents were added to the cells and incubated at 37 °C. The absorbance at 450 nm was read within 1 h. The concentrations required to inhibit cell growth by 50% (GI_{50}) were calculated using GraphPad Prism version 3.0 by nonlinear data fitting.

2.10. Data analysis

The net water flux in the mouse perfusion studies was determined using phenol red (14 μM), a non-absorbed and non-metabolized marker. The measured C_{out}/C_{in} ratio of test compound was corrected for water flux according to the following equation:

$$\frac{C'_{\text{out}}}{C'_{\text{in}}} = \frac{C_{\text{out}}}{C_{\text{in}}} \times \frac{C_{\text{in phonol red}}}{C_{\text{out phenol red}}}$$

where $C_{\text{in phenol red}}$ and $C_{\text{out phenol red}}$ are equal to the concentration of phenol red in the inlet and the outlet samples, respectively. The effective permeability (P_{eff}; cm/s) through the mouse intestinal wall in the single-pass intestinal perfusion studies was determined according to the following equation:

$$P_{eff} = \frac{-Q \ln\left(\frac{C'_{out}}{C'_{in}}\right)}{2\pi RL}$$

where Q is the perfusion buffer flow rate (0.08 mL/min), C'_{out}/C'_{in} is the ratio of the outlet/inlet concentration of test compound that is adjusted for water transport, R is the radius of the intestinal segment (set to 0.1 cm), and L is the length of the perfused intestinal segment.

2.11. HPLC analysis

The stability samples, cell permeated amounts of prodrugs and their metabolites, and perfusion samples were determined on an Agilent HPLC system (Agilent Technologies, Santa Clara, CA). The HPLC system consisted of Agilent pumps (1100 series), an Agilent autosampler (1200 series), and an Agilent UV–Vis detector (1100 series) controlled by Chemstation® 32 software (version B.01.03). Samples were resolved in an Agilent Eclipse Plus C18 reverse-phase column (3.5 μm, 4.6 × 75 mm) equipped with a guard column. The mobile phase consisted of 0.1% TFA/water (Solvent A) and 0.1% TFA/acetonitrile (Solvent B) with the solvent B gradient changing from 0% to 56% at a rate of 2%/min during a 15 min run for gemcitabine and gemcitabine prodrugs. Standard curves generated for each prodrug and their parent drug were utilized for quantitation of integrated area under peaks. The detection wavelength was 254 nm and spectra were acquired in the 220–380 nm wavelength range. The detection wavelength for phenol red was 430 nm.

2.12. LC–MS analysis

The LC–MS analytical method of 5′-mono-amino acid ester pro-drugs of floxuridine has been reported previously [41]. The LC–MS analysis of amino acid monoester prodrugs of gemcitabine was modified and performed in a similar manner. Briefly, LC–MS analysis of the uptake drug amount was performed in triplicate on LCMS-2010EV (Shimadzu Scientific Instruments, Kyoto, Japan) equipped with an ESI (electrospray ionization) source. The Shimadzu LC–MS system consisting of Shimadzu LC-20AD pumps with DGU-20A in-line vacuum degasser units, and SIL-20A HT autosam-pler with a Hypercarb column, 2.1 × 100 mm, 5 μm particle size (Thermo Scientific) was used for the separation and the effluent from the column was introduced directly to the ionization source. The system was controlled by Shimadzu LCMS solution software (version 3) to collect and process data. All samples were run with Solvent A and Solvent B (described earlier) with Solvent B gradient changing from 0% to 90% at a rate of 13.8%/min over a 22 min run. The ESI probe was operated with a detector voltage of 1.5 kV, CDL temperature of 250 °C, heat block of 200 °C, and nebulizing gas flow of 1.2 mL/min in positive mode for gemcitabine prodrugs and their metabolites. The drying gas was N2 delivered at 0.1 MPa.

2.13. Statistical analysis

Statistical analysis was performed by Student's *t*-test for two groups. All results were expressed as the mean ± standard deviation (SD). A probability (p) of less than 0.05 is considered statistically significant.

3. Results

3.1. Gemcitabine prodrugs

The synthesis of gemcitabine prodrugs, the evaluation of pro-drug purity by HPLC, NMR condition, and their characterization have been described in the previous report [5]. The structures and analytical data of those prodrugs are shown in Fig. 1 and Table 1.

3.2. The stability of gemcitabine and gemcitabine prodrugs in SGF, SIF (pH 6.5), phosphate buffer (pH 7.4), Caco-2 and AsPC-1 cell homogenates, human liver microsomes and thymidine phosphorylase enzyme

The experiments concerning prodrug stability were performed at 37 °C in pH 7.4 phosphate buffer. The estimated half-lives ($t_{1/2}$) obtained from linear regression of pseudo-first-order plots of pro-drug concentration vs. time for gemcitabine prodrugs in SGF, SIF (pH 6.5), pH 7.4 phosphate buffers alone, human liver microsomes, thymidine phosphorylase enzyme and in Caco-2 and AsPC-1 cell homogenates are listed in Table 2. Prodrug metabolites such as gemcitabine, 2′-deoxy-2′,2′-difluorouridine, uracil, and cytosine were monitored along with prodrug disappearance in this experiment. However, the mass balance could not be established because cytosine and uracil were metabolized even further and those metabolites could not be quantified by HPLC. All tested prodrugs and their parent drug did not show the significant degradation in SGF and SIF and exhibited more than 2 h of half-lives in pH 7.5 phosphate buffer. 5′-D-phenylalanyl-gemcitabine exhibited the highest stability for prodrugs and gemcitabine exhibited no significant degradation in SGF, SIF, and pH 7.4 phosphate buffer. All pro-drugs and gemcitabine exhibited 1.1–60.0-fold shorter half-lives in cell homogenates than in pH 7.4 phosphate buffer suggesting enzyme-catalyzed hydrolysis. The composition of the amino acids (L- and D-) in the promoiety exerted a profound effect on the stability of the ester bond. The stability of 5′-D-valyl-gemcitabine pro-drug was 2.2- and 6.3-fold better enzymatically in cell homogenates than one of 5′-L-valyl-gemcitabine prodrug, while the stability of 5′-D-phenylalanyl-gemcitabine prodrug was also 9.4- and 10.9-fold better enzymatically in cell homogenates than one of 5′-L-phenylalanyl-gemcitabine prodrug. In human liver microsomes, 5′-D-phenylalanyl-gemcitabine prodrug exhibited 3.7-fold better stability than one of 5′-L-phenylalanyl-gemcitabine prodrug, while valyl-gemcitabine prodrugs did not exhibit much difference. All prodrugs exhibited the resistance against the thymi-dine phosphorylase, while their parent drug, gemcitabine, did not display the resistance to this enzyme (Table 2).

3.3. Uptake study of gemcitabine and gemcitabine prodrugs in Caco-2 and AsPC-1 cells

The uptake of mono-amino acid monoester prodrugs of gemcit-abine and parent gemcitabine was determined with both the presence and the absence of 10 mM Gly-Pro at 37 °C in Caco-2 and AsPC-1 cells. Fig. 2 and Table 3 show the uptake amounts with observed compound species and the uptake difference with both the presence and the absence of 10 mM Gly-Pro in Caco-2 cell system. Fig. 3 shows the uptake amounts with two different drug concentrations and Table 4 shows observed compound species in AsPC-1, a ductal pancreatic cancer cell line, cell system. All ester prodrugs of gemcitabine exhibited 1.2–18.1-fold higher uptake amount than gemcitabine in Caco-2 and AsPC-1 cells except the uptake study with the lower concentration of 5′-D-phenylalanyl-gemcitabine prodrug in

AsPC-1 cells, which did not show the enhancement of uptake to gemcitabine. The uptake amounts of 5′-D-valyl-gemcitabine prodrug and 5′-D-phenylalanyl-gemcitabine prodrug were 3.1-fold and 3.3-fold higher in AsPC-1 cells than ones of 5′-L-valyl-gemcitabine prodrug and 5′-L-phenylalanyl-gemcita-bine prodrug with 100 μM drug solution (Fig. 3A). The uptake studies in AsPC-1 cells with lower drug solution (50 μM) exhibited the same trend in valyl-gemcitabine prodrugs but not in phenylal-anyl-gemcitabine prodrug (Fig. 3B). The dose linearity of gemcita-bine prodrug uptake in AsPC-1 cells was not clear ($R^2 = 0.15$) even though 5′-D-valyl-gemcitabine prodrug exhibited the dose linearity in uptake studies (Fig. 4). Gemcitabine and gemcitabine prodrugs with L-configuration amino acids exhibited the similar uptake amounts regardless of starting drug concentration for the study. The uptake amounts of 5′-D-valyl-gemcitabine prodrug and 5′-D-phenylalanyl-gemcitabine prodrug were 46% and 70% lower in Caco-2 cells than ones of 5′-L-valyl-gemcitabine prodrug and 5′-L-phenylalanyl-gemcitabine prodrug. Gemcitabine prodrugs exhibited 5.4–18.1-fold higher uptake amounts in Caco-2 cells than gemcitabine. Gemcitabine did not exhibit the difference in the uptake amount in Caco-2 cells with the presence and the absence of 10 mM Gly-Pro. The uptake amounts of gemcitabine prodrugs in Caco-2 cells were reduced 1.2–10.6-fold with the presence of 10 mM Gly-Pro compared with ones with the absence 10 mM Gly-Pro, suggesting that the improved cellular uptake of gemcita-bine prodrugs attributes to transporters at Caco-2 cells.

3.4. Caco-2 cell permeability of gemcitabine and gemcitabine prodrugs

The apical-to-basolateral permeability of mono-amino acid monoester prodrugs of gemcitabine and parent gemcitabine was determined with the presence and the absence of 10 mM Gly-Pro at 37 °C in Caco-2 cell monolayers. Table 5 and Fig. 5 show the permeability values and the permeability difference in this cell system. All monoester prodrugs of gemcitabine exhibited 3.8–4.5-fold higher permeability than gemcitabine in Caco-2 cells. Gemcitabine did not exhibit the difference in the membrane permeability with the presence and the absence of 10 mM Gly-Pro. The permeability of gemcitabine prodrugs across Caco-2 monolayers was 1.6–6.5-fold lower with the presence of 10 mM Gly-Pro than one without 10 mM Gly-Pro, suggesting that the improved permeability of gemcitabine prodrugs is attributed to transporters such as a PEPT1 transporter at Caco-2 monolayers.

3.5. In situ permeability in the single-pass intestinal perfusion study and the drug concentration in plasma in mice

The effective permeability (P_{eff}) values obtained for gemcitabine prodrugs and gemcitabine in small intestinal segments in mice at physiological pH are presented in Table 5. The *in situ* permeability of parent drug, gemcitabine, exhibited 2.0×10^{-6} cm/s in the mouse jejunum. On the other hand, the *in situ* permeability of (D-/L-) amino acid monoester prodrugs of gemcitabine exhibited 9.6–17.9-fold higher membrane permeability than their parent drug, gemcitabine. Gemcitabine prodrugs with L-amino acid exhibited superior membrane permeability to gemcitabine prodrugs with D-amino acid. 5′-L-valyl-gemcitabine prodrug and 5′-L-phen-ylalanyl-gemcitabine prodrug exhibited 87% and 56% better membrane permeability than 5′-D-valyl-gemcitabine prodrug and 5′-D-phenylalanyl-gemcitabine prodrug, respectively. In plasma samples following *in situ* perfusion, all prodrugs exhibited 1.3–9.8-fold higher concentration of prodrugs including their metabolites, gemcitabine and

cytosine, than their parent drug, gemcitabine. 5′-D-valyl-gemcitabine prodrug and 5′-D-phenylalanyl-gemcitabine prodrug exhibited 2.3-fold and 2.0-fold higher concentration in the plasma than 5′-L-valyl-gemcitabine prodrug and 5′-L-phenylalanyl-gemcitabine prodrug, even though the permeability numbers of gemcitabine prodrugs with D-form amino acids were lower than ones with L-form amino acid (Fig. 6). Furthermore, 5′-D-valyl-gemcitabine prodrug and 5′-D-phenylalanyl-gemcitabine prodrug appeared more prodrug forms in the plasma than 5′-L-valyl-gemcitabine prodrug and 5′-L-phenylalanyl-gemcitabine prodrug, suggesting that the D-amino acid mono-ester prodrugs of gemcitabine improved their stability toward metabolic enzymes.

3.6. Cell proliferation assay

GI_{50} values for gemcitabine and gemcitabine prodrugs, 5′-amino acid monoester prodrugs of gemcitabine, determined in cell proliferation studies with the pancreatic ductal cell line, AsPC-1, are shown in Table 6. All prodrugs exhibited 1.8–5.1-fold enhanced antiproliferative activity in the cancer cell line compared to their parent, gemcitabine. Valyl-gemcitabine (L- and D-) exhibited 2.0–2.8-fold better growth inhibitory effects than phenylalanyl-gemcitabine (L- and D-). Thus, the GI_{50} values of all gemcitabine prodrugs were in the range of 2.0–5.6 mM in AsPC-1 cell as opposed to GI_{50} value of 10.2 mM for gemcitabine in AsPC-1 cell. D-Form amino acid attached gemcitabine prodrugs exhibited a slightly inferior antiproliferative activity to L-form amino acid attached gemcitabine.

4. Discussion

Amino acid ester prodrugs have been widely employed to improve intestinal absorption of poorly permeable drugs. The antivirals valacyclovir and valganciclovir are early examples for the success of amino acid ester prodrug strategies [21,42]. The improved oral bioavailability of these anti-virals has been attributed to their enhanced affinity to transporters [3,4,43–45]. A variety of amino acid, dipeptide and tripeptide have been investigated to improve the oral absorption via intake transporters as a part of prodrug approaches [16,17,22–24,46–49]. We have synthesized mono-amino acid and dipeptide prodrugs of floxuridine, gemcita-bine and 2-bromo-5,6- dichloro-1-(beta-d-ribofuranosyl) benz-imidazole (BDCRM) and characterized their stability and membrane permeability [5,6,9–11,13,14,30,50]. These studies revealed that mono-amino acid/dipeptide ester prodrugs in general enhance the PEPT1-mediated transport and glycosidic bond resistance to metabolic enzymes such as thymidine phosphorylase and cytidine deaminase. In this report, we describe the chemical and enzymatic stability and bioactivation of mono-amino acid monoester prodrugs of gemcitabine in buffer, Caco-2 cells, a surrogate for intestine, AsPC-1 cells, a surrogate for tumor, liver micro-somes and the enzyme, thymidine phosphorylase. We conducted uptake studies in Caco-2 and AsPC-1 cells to evaluate the transport. We also performed transepithelial studies with Caco-2 monolayers and *in situ* perfusion studies in mice to calculate the membrane permeability along with the drug concentration in plasma for the evaluation of oral drug delivery for pancreatic cancer treatment.

The mono-amino acid prodrugs of gemcitabine appeared to be relatively stable in pH 7.4 buffers and exhibited more stable in acidic pH, SGF and SIF (pH 6.5), which agreed with our previous results [30]. The enzymatic stability of 5′-D-phenylalanyl-gemcita-bine and 5′-

D-valyl-gemcitabine was significantly enhanced compared to ones of 5′-L-phenylalanyl-gemcitabine and 5′-L-va-lyl-gemcitabine suggesting that the recognition of enzymes to their substrates is specific and, hence, the unnatural form of amino acids such as D-valine and D-phenylalanine decelerates enzyme-catalyzed hydrolysis of the ester linkage. The stability profiles of 5′-D-phenylalanyl-gemcitabine and 5′-D-valyl-gemcitabine in cell homogenates, Caco-2 and AsPC-1, liver microsomes, and thymi-dine phosphorylase suggest that activation of D-amino acid mono-ester prodrug to the parent drug following transport would be much slower than activation of L-amino acid monoester prodrugs, 5′-L-valyl-gemcitabine and 5′-L-phenylalanyl-gemcitabine. The improved stability in biological surrogate media would facilitate prolonged systemic circulation of intact prodrugs and, hence, target delivery to the cancer sites for enhanced therapeutic action. The plasma concentration of D-amino acid monoester prodrug forms of gemcitabine after their *in situ* perfusion in mice was higher than one of L-amino acid monoester prodrug forms of gemcita-bine (Fig. 6).

The results of the uptake studies of the amino acid monoester prodrugs in Caco-2 and AsPC-1 are shown in Figs. 2 and 3 and Tables 3 and 4. The uptake amounts of gemcitabine prodrugs were consistently lower in AsPC-1 cells compared to their corresponding values in Caco-2 cells. Gemcitabine was degraded almost three times faster in AsPC-1 cells than in Caco-2 cells. Those indicate that prodrug stability and enzyme upregulation in AsPC-1 cells would be largely attributed to the observed uptake amount for gemcitabine prodrugs and their metabolites. The noticeable difference between those results was the trend of uptake amount. Gemcitabine prodrugs with L-amino acid exhibited higher uptake amount in Caco-2 cells than ones with D-amino acid. On the other hand, gemcitabine prodrugs with D-amino acid exhibited higher uptake amount in AsPC-1 cells than ones with L-amino acid. Those uptake results exhibited different pattern of drug species, gemcitabine prodrug, gemcitabine, and cytosine, in those two cell lines. The uptake of gemcitabine prodrugs in Caco-2 uptake exhibited 69–90% of prodrug form, 10–31% of gemcitabine and 0% of cytosine, while the uptake of gemcitabine prodrugs in AsPC-1 exhibited 6–69% of prodrug form, 11–87% of gemcitabine and 1–20% of cytosine. Those results suggest that the expression level of metabolizing enzymes for gemcitabine prodrugs and gemcitabine in those cells was different, the substrate recognition of enzymes was specific depending on the configuration amino acid, and, as a result, the bioactivation rate of those prodrugs was different. Thus, attachment of the D-configuration amino acid to gemcitabine yielded 2–10-fold improved stability for enzymatic degradation even though it lowered the affinity to transporters. The intake transporter, PEPT1, has a broad substrate specificity with a low-affinity (Km of 200 μM to 15 mM) and high capacity, and recognizes D-configuration amino acid promoiety as a substrate [27,51]. The interactions between transporters and prodrugs and between activation enzymes and prodrugs are different as each prodrug possesses unique binding affinity and rates to those transporters and enzymes [52]. With the complexity of those processes, the meaningful dose linearity ($R^2 = 0.15$) in uptake studies for gemcitabine and gemcitabine prodrugs in AsPC-1 cells was not observed even though those studies were carried out below their Km values (Fig. 4).

The apical-to-basolateral permeability of mono-amino acid monoester prodrugs of gemcitabine and their parent drug, gemcitabine, were determined at 37 °C in Caco-2 cell

monolayer with both the presence and the absence of Gly-Pro (Fig. 5). The prodrug permeability across Caco-2 cell monolayer was reduced with the presence of Gly-Pro, while the permeability of gemcitabine did not change with the presence and the absence of Gly-Pro. Thus, the improved permeability of the mono-amino acid monoester prodrugs across Caco-2 cell monolayer indicates enhanced transporter-mediated transport of gemcitabine prodrugs. The detection of only cytosine in the basolateral receiver compartment following transport of gemcitabine across Caco-2 monolayers suggests the instability of the glycosidic bond. The conversion of prodrugs to cytosine following transport was substantially lower in Caco-2 cells, especially for 5′-D-valyl-gemcitabine and 5′-D-phenylalanyl-gemcitabine. The average percent cytosine in the basolateral compartment was observed 76% (the range 61–92%) in Caco-2 monolayer studies (data not shown). In general, conversion of gemcitabine prodrugs with D-amino acid to cytosine following transport across the monolayers was about 1.4-fold lower than that observed with L-amino acid ester prodrugs of gemcitabine. The results are consistent with stability profiles of gemcitabine prodrugs in the presence of thymidine phosphorylase, an enzyme involved in the *in vivo* for phosphorytic cleavage of gemcitabine [53]. P_{eff} values of gemcitabine prodrugs were 9- and 18-fold higher than one of gemcitabine (Table 5). The effective permeability (P_{eff}) values of the gemcitabine prodrugs as well as parent gemcit- abine in mouse jejunal intestine are consistent with the trends observed in uptake studies in Caco-2 cells and the excellent correlation between those two was observed ($R^2 = 0.87$) (Fig. 7). In the previous studies with mono-amino acid prodrugs of floxuridine, our group has demonstrated the excellent linear correlations between Caco-2 permeability and PEPT1-mediated transport in HeLa/PEPT1 cells [54].

Gemcitabine was rapidly cleaved by thymidine phosphorylase but all amino acid ester prodrugs examined in this study were more stable toward thymidine phosphorylase (Table 2). The esterification of 5′-hydroxyl groups would protect the glycosidic bond cleavage by thymidine phosphorylase, which has been discussed in previous studies [9,13].

The cell proliferation studies in the pancreatic ductal cancer cell line confirmed the enhanced potency of the amino acid ester pro-drugs compared to their parent gemcitabine. The results of uptake study in AsPC-1 cell suggested that the enhanced antiproliferative effect on cancer cells attributed the improved membrane permeability of gemcitabine prodrugs. Mono-amino acid monoester pro-drugs of gemcitabine exhibited better GI_{50} values compared to one of gemcitabine. The GI_{50} values of prodrugs did not exhibit any discernible correlations with their uptake values in AsPC-1 cells. Since the bioconversion rate of prodrugs will be various according to their different (D-/L-) amino acid promoieties, the time after transport into cancer cells to reach their maximum antiproliferative activity will be different [52]. Therefore, it would be difficult to distinguish a significant correlation between GI_{50} values and prodrug permeabilities with a limited experimental time course.

5. Conclusion

Intracellular anabolism of gemcitabine prodrugs may illustrate that transported drugs are converted to gemcitabine and cytosine via a sequential enzymatic pathway including the high expression of thymidine phosphorylase in tumor cells (Tables 3 and 4). The gemcitabine prodrugs with D-configuration amino acids demonstrated the superior stability

against metabolic enzymes. As a result, those prodrugs would exhibit higher concentration of cancer drugs in systemic circulation after *in situ* perfusion of mouse small intestine even though those prodrugs have inferior affinity for transporters compared to gemcitabine prodrugs with L-configuration amino acids. Even though those gemcitabine prodrugs with D-configuration amino acids showed some potential to develop the oral dosage forms for cancer, oral bioavailability of those pro-drugs has to be determined by another set of experiment to evaluate their potentials. Our results indicate that (D-/L-) amino acid monoester prodrugs of gemcitabine exhibit significantly higher permeability in Caco-2 cell monolayer and mouse intestinal membrane than their parent drug, gemcitabine, suggesting their potential for the development of oral dosage form for anti-cancer nucleoside analogs. Especially, gemcitabine prodrugs with D-con-figuration amino acids exhibited higher prodrug concentration in systemic circulation after *in situ* perfusion of mouse small intestine. Therefore, prodrugs with D-configuration amino acids might possess advantages over prodrugs with L-configuration amino acids for the development of oral dosage form. Gemcitabine pro-drug, 5′-D-valyl-gemcitabine, displayed significantly higher permeability in Caco-2 cell monolayer and mouse intestinal membrane and highest prodrug concentration in blood with improved antiproliferative activity against pancreatic ductal cancer cells, AsPC-1. The enhanced metabolic resistance, the higher prodrug concentration in plasma after oral absorption, and the improved anti-cancer effect may facilitate the development of oral dosage form for pyrimidine analogues such as gemcitabine and floxuridine to treat cancer. The successful development of oral dosage form for cancer therapeutic agents will vastly improve the quality of life for cancer patients due to its convenient chemotherapy.

Acknowledgments

This work was supported by Grants NIGMD-2R01GM037188.

Abbreviations

Gly-Pro	Glycine-Proline
P_{aap}	apparent permeability
P_{eff}	effective permeability

References

1. van Moorsel CJ, Peters GJ, Pinedo HM. Gemcitabine: future prospects of single-agent and combination studies. Oncologist. 1997; 2:127–134. [PubMed: 10388042]
2. Zhang Y, Kim WY, Huang L. Systemic delivery of gemcitabine triphosphate via LCP nanoparticles for NSCLC and pancreatic cancer therapy. Biomaterials. 2013; 34:3447–3458. [PubMed: 23380359]
3. Han H, de Vrueh RL, Rhie JK, Covitz KM, Smith PL, Lee CP, Oh DM, Sadee W, Amidon GL. 5′-Amino acid esters of antiviral nucleosides, acyclovir, and AZT are absorbed by the intestinal PEPT1 peptide transporter. Pharm Res. 1998; 15:1154–1159. [PubMed: 9706043]
4. Han HK, Oh DM, Amidon GL. Cellular uptake mechanism of amino acid ester prodrugs in Caco-2/hPEPT1 cells overexpressing a human peptide transporter. Pharm Res. 1998; 15:1382–1386. [PubMed: 9755889]

5. Song X, Lorenzi PL, Landowski CP, Vig BS, Hilfinger JM, Amidon GL. Amino acid ester prodrugs of the anticancer agent gemcitabine: synthesis, bioconversion, metabolic bioevasion, and hPEPT1-mediated transport. Mol Pharm. 2005; 2:157–167. [PubMed: 15804190]
6. Song X, Vig BS, Lorenzi PL, Drach JC, Townsend LB, Amidon GL. Amino acid ester prodrugs of the antiviral agent 2-bromo-5,6-dichloro-1-(beta-D-ribofuranosyl)benzimidazole as potential substrates of hPEPT1 transporter. J Med Chem. 2005; 48:1274–1277. [PubMed: 15715497]
7. Talluri RS, Samanta SK, Gaudana R, Mitra AK. Synthesis, metabolism and cellular permeability of enzymatically stable dipeptide prodrugs of acyclovir. Int J Pharm. 2008; 361:118–124. [PubMed: 18573320]
8. Tolle-Sander S, Lentz KA, Maeda DY, Coop A, Polli JE. Increased acyclovir oral bioavailability via a bile acid conjugate. Mol Pharm. 2004; 1:40–48. [PubMed: 15832499]
9. Tsume Y, Hilfinger JM, Amidon GL. Enhanced cancer cell growth inhibition by dipeptide prodrugs of floxuridine: increased transporter affinity and metabolic stability. Mol Pharm. 2008; 5:717–727. [PubMed: 18652477]
10. Tsume Y, Vig BS, Sun J, Landowski CP, Hilfinger JM, Ramachandran C, Amidon GL. Enhanced absorption and growth inhibition with amino acid monoester prodrugs of floxuridine by targeting hPEPT1 transporters. Molecules. 2008; 13:1441–1454. [PubMed: 18719516]
11. Vig BS, Lorenzi PJ, Mittal S, Landowski CP, Shin HC, Mosberg HI, Hilfinger JM, Amidon GL. Amino acid ester prodrugs of floxuridine: synthesis and effects of structure, stereochemistry, and site of esterification on the rate of hydrolysis. Pharm Res. 2003; 20:1381–1388. [PubMed: 14567631]
12. Kawaguchi T, Saito M, Suzuki Y, Nambu N, Nagai T. Specificity of esterases and structure of prodrug esters. II. Hydrolytic regeneration behavior of 5-fluoro-2′-deoxyuridine (FUdR) from 3′, 5′-diesters of FUdR with rat tissue homogenates and plasma in relation to their antitumor activity. Chem Pharm Bull (Tokyo). 1985; 33:1652–1659. [PubMed: 2931191]
13. Landowski CP, Song X, Lorenzi PL, Hilfinger JM, Amidon GL. Floxuridine amino acid ester prodrugs: enhancing Caco-2 permeability and resistance to glycosidic bond metabolism. Pharm Res. 2005; 22:1510–1518. [PubMed: 16132363]
14. Landowski CP, Vig BS, Song X, Amidon GL. Targeted delivery to PEPT1-overexpressing cells: acidic, basic, and secondary floxuridine amino acid ester prodrugs. Mol Cancer Ther. 2005; 4:659–667. [PubMed: 15827340]
15. Nishizawa Y, Casida JE. 3′,5′-Diesters of 5-fluoro-2′-deoxyuridine: synthesis and biological activity. Biochem Pharmacol. 1965; 14:1605–1619. [PubMed: 4222443]
16. Anand BS, Patel J, Mitra AK. Interactions of the dipeptide ester prodrugs of acyclovir with the intestinal oligopeptide transporter: competitive inhibition of glycylsarcosine transport in human intestinal cell line-Caco-2. J Pharmacol Exp Therap. 2003; 304:781–791. [PubMed: 12538834]
17. Friedrichsen GM, Chen W, Begtrup M, Lee CP, Smith PL, Borchardt RT. Synthesis of analogs of L-valacyclovir and determination of their substrate activity for the oligopeptide transporter in Caco-2 cells. Eur J Pharm Sci. 2002; 16:1–13. [PubMed: 12113886]
18. Guo A, Hu P, Balimane PV, Leibach FH, Sinko PJ. Interactions of a nonpeptidic drug, valacyclovir, with the human intestinal peptide transporter (hPEPT1) expressed in a mammalian cell line. J Pharmacol Exp Therap. 1999; 289:448–454. [PubMed: 10087037]
19. Hatanaka T, Haramura M, Fei YJ, Miyauchi S, Bridges CC, Ganapathy PS, Smith SB, Ganapathy V, Ganapathy ME. Transport of amino acid-based prodrugs by the Na+- and Cl(−)-coupled amino acid transporter ATB0,+ and expression of the transporter in tissues amenable for drug delivery. J Pharmacol Exp Therap. 2004; 308:1138–1147. [PubMed: 14617696]
20. Phan DD, Chin-Hong P, Lin ET, Anderle P, Sadee W, Guglielmo BJ. Intra-and interindividual variabilities of valacyclovir oral bioavailability and effect of coadministration of an hPEPT1 inhibitor. Antimicrob Agents Chemother. 2003; 47:2351–2353. [PubMed: 12821497]
21. Umapathy NS, Ganapathy V, Ganapathy ME. Transport of amino acid esters and the amino-acid-based prodrug valganciclovir by the amino acid transporter ATB(0,+). Pharm Res. 2004; 21:1303–1310. [PubMed: 15290873]

22. Anand BS, Katragadda S, Mitra AK. Pharmacokinetics of novel dipeptide ester prodrugs of acyclovir after oral administration: intestinal absorption and liver metabolism. J Pharmacol Exp Therap. 2004; 311:659–667. [PubMed: 15226381]
23. Meredith D, Temple CS, Guha N, Sword CJ, Boyd CA, Collier ID, Morgan KM, Bailey PD. Modified amino acids and peptides as substrates for the intestinal peptide transporter PepT1. Eur J Biochem. 2000; 267:3723–3728. [PubMed: 10848990]
24. Nielsen CU, Andersen R, Brodin B, Frokjaer S, Taub ME, Steffansen B. Dipeptide model prodrugs for the intestinal oligopeptide transporter. Affinity for and transport via hPepT1 in the human intestinal Caco-2 cell line. J Control Release. 2001; 76:129–138. [PubMed: 11532319]
25. Satake M, Enjoh M, Nakamura Y, Takano T, Kawamura Y, Arai S, Shimizu M. Transepithelial transport of the bioactive tripeptide, Val-Pro-Pro, in human intestinal Caco-2 cell monolayers. Biosci Biotechnol Biochem. 2002; 66:378–384. [PubMed: 11999412]
26. Surendran N, Covitz KM, Han H, Sadee W, Oh DM, Amidon GL, Williamson RM, Bigge CF, Stewart BH. Evidence for overlapping substrate specificity between large neutral amino acid (LNAA) and dipeptide (hPEPT1) transporters for PD 158473, an NMDA antagonist. Pharm Res. 1999; 16:391–395. [PubMed: 10213369]
27. Wenzel U, Gebert I, Weintraut H, Weber WM, Clauss W, Daniel H. Transport characteristics of differently charged cephalosporin antibiotics in oocytes expressing the cloned intestinal peptide transporter PepT1 and in human intestinal Caco-2 cells. J Pharmacol Exp Therap. 1996; 277:831–839. [PubMed: 8627565]
28. Wenzel U, Thwaites DT, Daniel H. Stereoselective uptake of beta-lactam antibiotics by the intestinal peptide transporter. Br J Pharmacol. 1995; 116:3021–3027. [PubMed: 8680738]
29. Rubio-Aliaga I, Daniel H. Mammalian peptide transporters as targets for drug delivery. Trends Pharmacol Sci. 2002; 23:434–440. [PubMed: 12237156]
30. Tsume Y, Hilfinger JM, Amidon GL. Potential of amino acid/dipeptide monoester prodrugs of floxuridine in facilitating enhanced delivery of active drug to interior sites of tumors: a two-tier monolayer in vitro study. Pharm Res. 2011; 28:2575–2588. [PubMed: 21671137]
31. Gonzalez DE, Covitz KM, Sadee W, Mrsny RJ. An oligopeptide transporter is expressed at high levels in the pancreatic carcinoma cell lines AsPc-1 and Capan-2. Cancer Res. 1998; 58:519–525. [PubMed: 9458100]
32. Garcia-Manteiga J, Molina-Arcas M, Casado FJ, Mazo A, Pastor-Anglada M. Nucleoside transporter profiles in human pancreatic cancer cells: role of hCNT1 in 2′,2′-difluorodeoxycytidine- induced cytotoxicity. Clin Cancer Res: An Off J Am Assoc Cancer Res. 2003; 9:5000–5008.
33. Grem JL. 5-Fluorouracil: forty-plus and still ticking. A review of its preclinical and clinical development. Invest New Drugs. 2000; 18:299–313. [PubMed: 11081567]
34. Kahramanogullari O, Fantaccini G, Lecca P, Morpurgo D, Priami C. Algorithmic modeling quantifies the complementary contribution of metabolic inhibitions to gemcitabine efficacy. PLoS ONE. 2012; 7:e50176. [PubMed: 23239976]
35. Veltkamp SA, Pluim D, van Eijndhoven MA, Bolijn MJ, Ong FH, Govindarajan R, Unadkat JD, Beijnen JH, Schellens JH. New insights into the pharmacology and cytotoxicity of gemcitabine and 2′,2′-difluorodeoxyuridine. Mol Cancer Ther. 2008; 7:2415–2425. [PubMed: 18723487]
36. O'Neill VJ, Twelves CJ. Oral cancer treatment: developments in chemotherapy and beyond. Br J Cancer. 2002; 87:933–937. [PubMed: 12434279]
37. Stuurman FE, Nuijen B, Beijnen JH, Schellens JH. Oral anticancer drugs: mechanisms of low bioavailability and strategies for improvement. Clin Pharmacokinet. 2013; 52:399–414. [PubMed: 23420518]
38. Birnie GD, Kroeger H, Heidelberger C. Studies of fluorinated pyrimidines. Xviii. The degradation of 5-fluoro-2′-deoxyuridine and related compounds by nucleoside phosphorylase. Biochemistry. 1963; 2:566–572. [PubMed: 14069549]
39. Bonastre J, Jan P, Barthe Y, Koscielny S. Metastatic breast cancer: we do need primary cost data. Breast. 2012; 21:384–388. [PubMed: 22520336]
40. Incecayir T, Tsume Y, Amidon GL. Comparison of the permeability of metoprolol and labetalol in rat, mouse, and Caco-2 cells: use as a reference standard for BCS classification. Mol Pharm. 2013

41. Tsume Y, Provoda CJ, Amidon GL. The achievement of mass balance by simultaneous quantification of floxuridine prodrug, floxuridine, 5-fluorouracil, 5-dihydrouracil, alpha-fluoro-beta-ureidopropionate, alpha-fluoro-beta-alanine using LC–MS. J Chromatogr B: Anal Technol Biomed Life Sci. 2011; 879:915–920.
42. Anand BS, Dey S, Mitra AK. Current prodrug strategies via membrane transporters/receptors. Expert Opin Biol Ther. 2002; 2:607–620. [PubMed: 12171505]
43. Ganapathy ME, Huang W, Wang H, Ganapathy V, Leibach FH. Valacyclovir: a substrate for the intestinal and renal peptide transporters PEPT1 and PEPT2. Biochem Biophys Res Commun. 1998; 246:470–475. [PubMed: 9610386]
44. Steingrimsdottir H, Gruber A, Palm C, Grimfors G, Kalin M, Eksborg S. Bioavailability of aciclovir after oral administration of aciclovir and its prodrug valaciclovir to patients with leukopenia after chemotherapy. Antimicrob Agents Chemother. 2000; 44:207–209. [PubMed: 10602752]
45. Weller S, Blum MR, Doucette M, Burnette T, Cederberg DM, de Miranda P, Smiley ML. Pharmacokinetics of the acyclovir pro-drug valaciclovir after escalating single- and multiple-dose administration to normal volunteers. Clin Pharmacol Ther. 1993; 54:595–605. [PubMed: 8275615]
46. Eriksson AH, Elm PL, Begtrup M, Nielsen R, Steffansen B, Brodin B. HPEPT1 affinity and translocation of selected Gln-Sar and Glu-Sar dipeptide derivatives. Mol Pharm. 2005; 2:242–249. [PubMed: 15934785]
47. Li J, Tamura K, Lee CP, Smith PL, Borchardt RT, Hidalgo IJ. Structure–affinity relationships of Val-Val and Val-Val-Val stereoisomers with the apical oligopeptide transporter in human intestinal Caco-2 cells. J Drug Target. 1998; 5:317–327. [PubMed: 9771614]
48. Tamura K, Bhatnagar PK, Takata JS, Lee CP, Smith PL, Borchardt RT. Metabolism, uptake, and transepithelial transport of the diastereomers of Val-Val in the human intestinal cell line, Caco-2. Pharm Res. 1996; 13:1213–1218. [PubMed: 8865315]
49. Vabeno J, Lejon T, Nielsen CU, Steffansen B, Chen W, Ouyang H, Borchardt RT, Luthman K. Phe-Gly dipeptidomimetics designed for the di-/ tripeptide transporters PEPT1 and PEPT2: synthesis and biological investigations. J Med Chem. 2004; 47:1060–1069. [PubMed: 14761208]
50. Lorenzi PL, Landowski CP, Song X, Borysko KZ, Breitenbach JM, Kim JS, Hilfinger JM, Townsend LB, Drach JC, Amidon GL. Amino acid ester prodrugs of 2-bromo-5,6-dichloro-1-(beta-D-ribofuranosyl)benzimidazole enhance metabolic stability in vitro and in vivo. J Pharmacol Exp Therap. 2005; 314:883–890. [PubMed: 15901797]
51. Cao F, Gao Y, Ping Q. Advances in research of PepT1-targeted prodrug. Asian J Pharm Sci. 2012; 7:110–122.
52. Tsume Y, Amidon GL. The feasibility of enzyme targeted activation for amino acid/dipeptide monoester prodrugs of floxuridine; cathepsin D as a potential targeted enzyme. Molecules. 2012; 17:3672–3689. [PubMed: 22450679]
53. Woodman PW, Sarrif AM, Heidelberger C. Specificity of pyrimidine nucleoside phosphorylases and the phosphorolysis of 5-fluoro-2′-deoxyuridine. Cancer Res. 1980; 40:507–511. [PubMed: 6451286]
54. Landowski CP, Lorenzi PL, Song X, Amidon GL. Nucleoside ester prodrug substrate specificity of liver carboxylesterase. J Pharmacol Exp Therap. 2006; 316:572–580. [PubMed: 16223870]

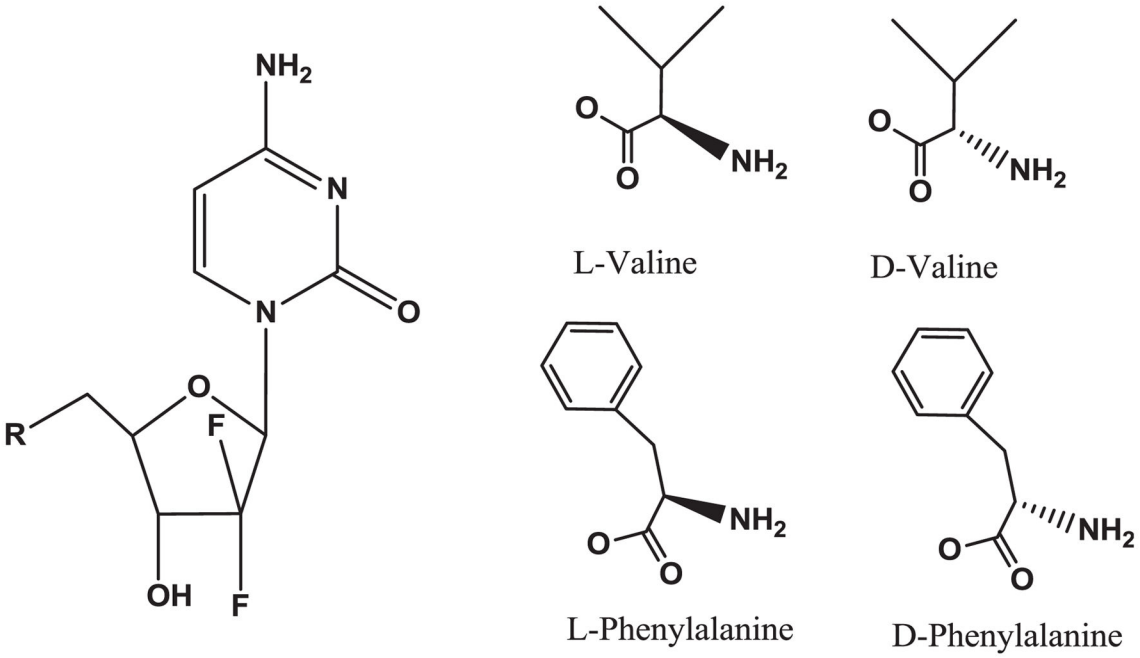

Fig. 1.
Amino acid monoester prodrugs of gemcitabine.

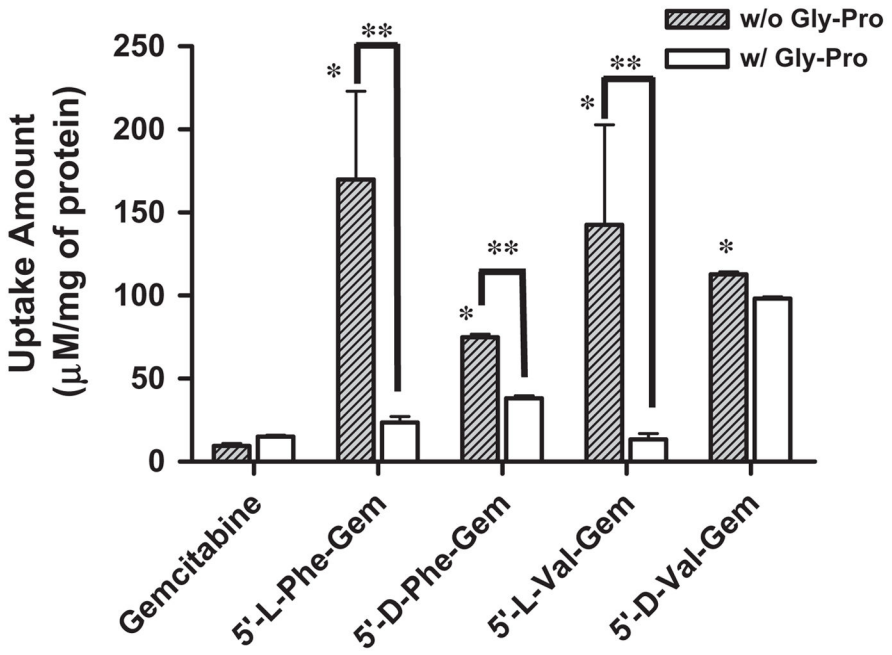

Fig. 2.

The amount of gemcitabine and gemcitabine prodrugs found in Caco-2 cells with 1 h incubation. Each column represents total amount of gemcitabine prodrug, gemcitabine, and cytosine. Data are expressed as the amount, μM/mg of protein, mean ± SD, $n = 3$. *$p < 0.05$, the uptake amount of gemcitabine prodrug is compared with gemcitabine's. $^{§}p < 0.05$, the uptake amount of gemcitabine prodrug is compared with one of the same prodrug with the presence of Gly-Pro.

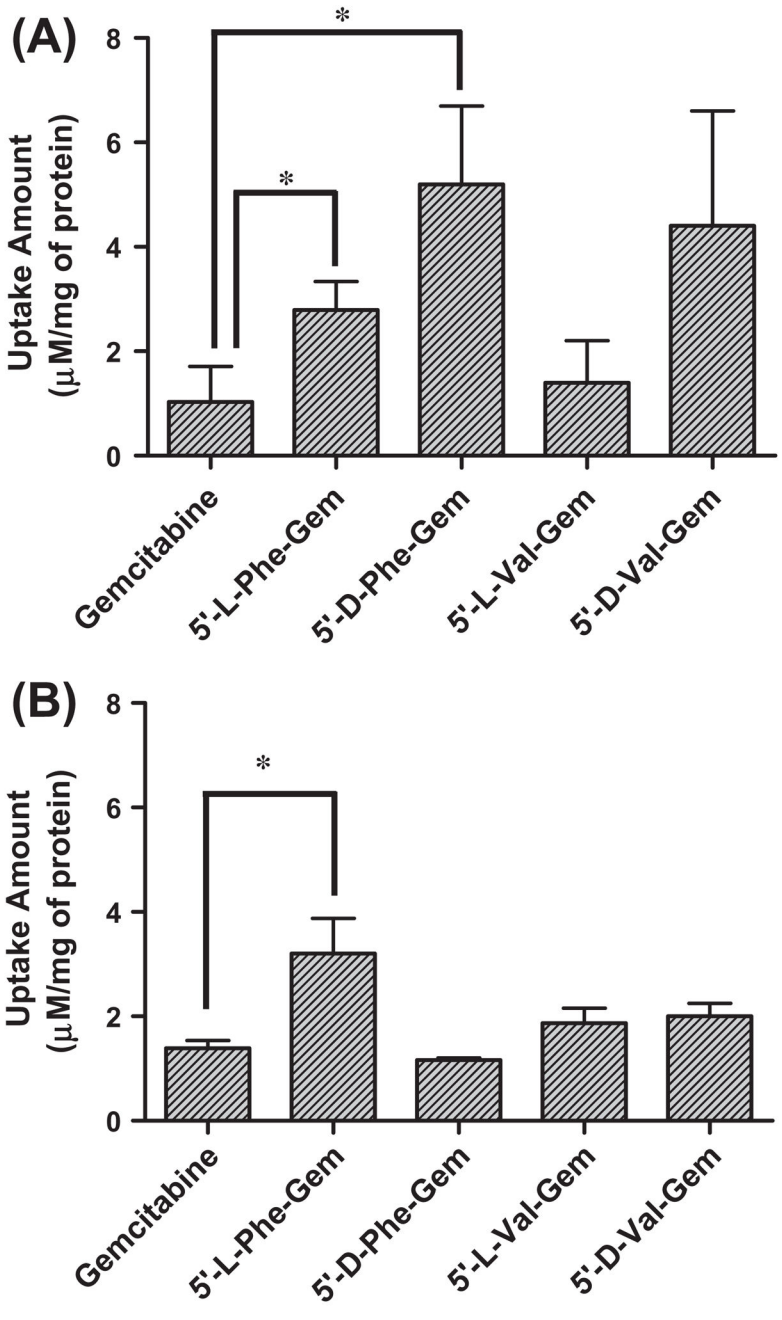

Fig. 3.

The amount of gemcitabine and gemcitabine prodrugs found in AsPC-1 with 1 h incubation; (A) 100 μM drug solution and (B) 50 μM drug solution. Each column represents the total amount of gemcitabine prodrug, gemcitabine, and cytosine. Data are expressed as the amount, μM/mg of protein, mean ± SD, $n = 3$. *$p < 0.05$, the uptake amount of gemcitabine prodrug is compared with gemcitabine's.

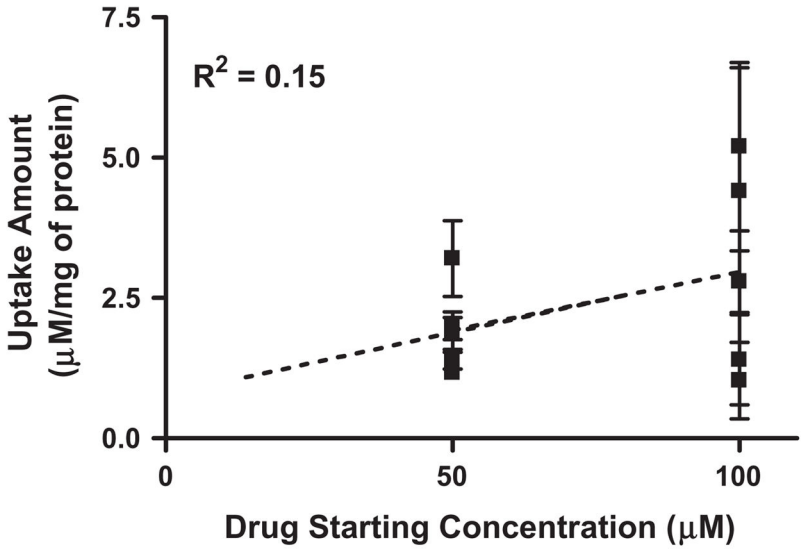

Fig. 4.

The correlation of uptake amount for gemcitabine and gemcitabine prodrugs in AsPC-1 cells between the starting concentration of 50 μM and the starting concentration of 100 μM. Values are the mean ± SD, $n = 3$.

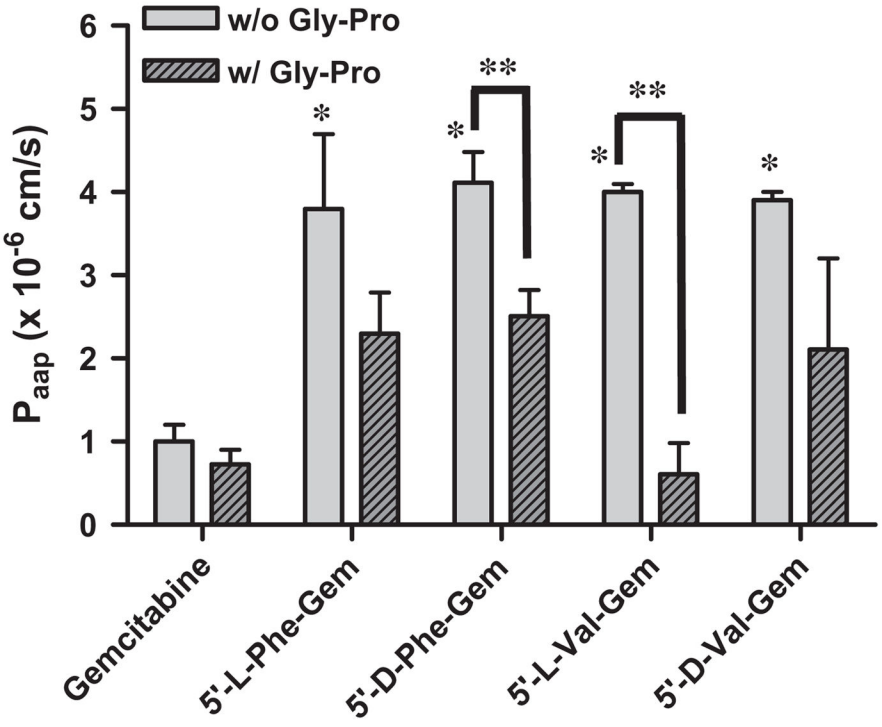

Fig. 5.

Apparent permeability coefficients (P_{app}) of gemcitabine and its amino acid ester prodrugs in the apical-to-basolateral direction across Caco-2 monolayer with the presence and the absence of Gly-Pro (mean ± SD, $n = 3$). *$p < 0.05$, the apparent permeability coefficient of gemcitabine prodrugs is compared with gemcitabine. **$p < 0.05$, the apparent permeability coefficient of gemcitabine and gemcitabine prodrugs is compared with one of the same drug with the presence of Gly-Pro.

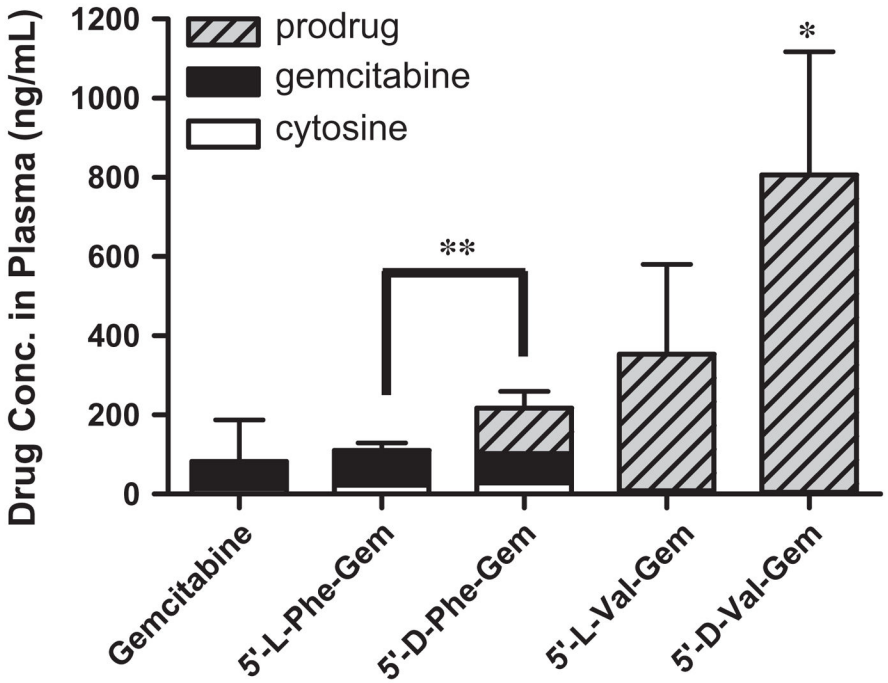

Fig. 6.

The concentration of gemcitabine and gemcitabine prodrugs found in plasma at 2 h following *in situ* single-pass intestinal perfusion to the mouse jejunum. Each column represents gemcitabine prodrug, gemcitabine, and cytosine. Data are expressed as the concentration, ng/mL, mean ± SD, $n = 3$. Error bars are shown for the total concentration. *$p < 0.05$, the drug concentration of 5′-D-Val-Gem is compared with gemcitabine. **$p < 0.05$, the drug concentration of 5′-L-enantiomers of amino acid prodrug is compared with one of D-enantiomers of amino acid prodrug.

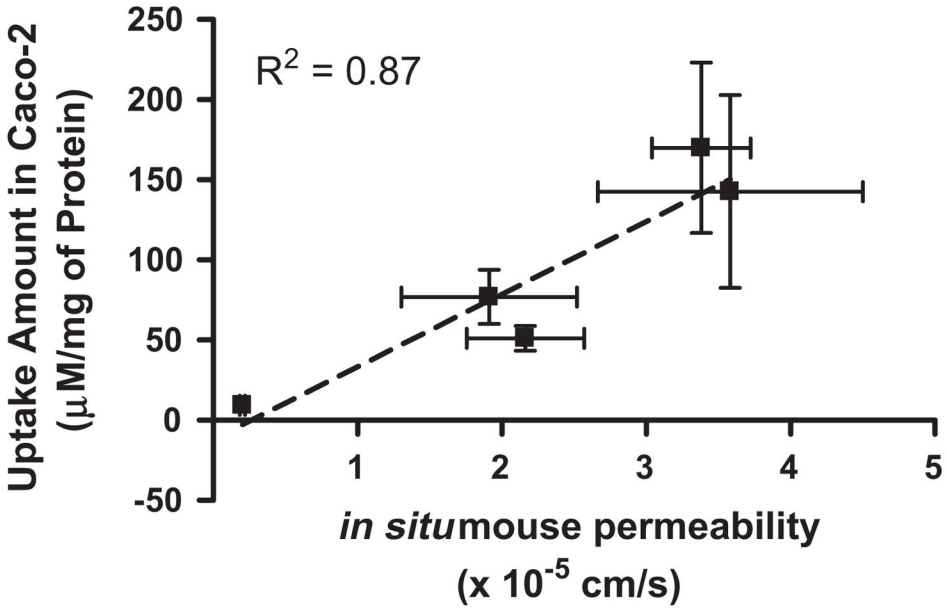

Fig. 7.

The correlation between the amount of gemcitabine and gemcitabine prodrugs in Caco-2 cells and the membrane permeabilities of gemcitabine and gemcitabine prodrugs in mouse jejunum. Values are the mean ± SD, *n* = 3.

Table 1

Analytical data for amino acid ester prodrugs of gemcitabine.

Prodrug	Purity (%) (HPLC)	ESI-MS $(M+H)^+$		CLogP[a]
		Required	Observed	
Gemcitabine	95.3	263.2	263.9	−0.71
5′-L-Phenylalanyl-gemcitabine (5′-L-Phe-Gem)	98.2	411.4	411.8	−0.36
5′-D-Phenylalanyl-gemcitabine (5′-D-Phe-Gem)	97.4	411.4	411.8	−0.36
5′-L-Valyl-gemcitabine (5′-L-Val-Gem)	98.1	363.3	364.0	−0.16
5′-D-Valyl-gemcitabine (5′-D-Phe-Gem)	98.6	363.3	364.0	−0.16

[a] Calculated using BioLoom.

Table 2

Stability of gemcitabine and gemcitabine prodrugs in pH 7.4 Buffer and biological media (mean ± SD, n = 3).

Prodrug	SGF $t_{1/2}$ (min)	SIF (pH 6.5) $t_{1/2}$ (min)	Buffer pH 7.4 $t_{1/2}$ (min)	Caco-2 cell homogenates $t_{1/2}$ (min)	Human liver microsome $t_{1/2}$ (min)	Thymidine phosphorylase $t_{1/2}$ (min)	AsPC-1 cell homogenates $t_{1/2}$ (min)
Gemcitabine	>120	>120	>120	105.0 ± 6.1	45.3 ± 3.3	6.0 ± 1.8	33.7 ± 14.5
5′-L-Phenylalanyl-gemcitabine	>120	>120	>120	2.0 ± 0.3	1.8 ± 0.2	31.9 ± 5.0	6.8 ± 2.0
5′-D-Phenylalanyl-gemcitabine	>120	>120	>120	21.7 ± 0.2	6.6 ± 1.3	>120	63.9 ± 11.2
5′-L-Valyl-gemcitabine	>120	>120	>120	19.5 ± 1.9	27.8 ± 13.6	>120	13.8 ± 3.3
5′-D-Valyl-gemcitabine	>120	>120	>120	42.0 ± 17.5	19.5 ± 4.4	>120	87.2 ± 13.5

Table 3

Composition of gemcitabine and gemcitabine prodrugs in Caco-2 cell uptake studies without Gly-Pro (mean ± SD, $n = 3$).

Compound	Cytosine (%)	Gemcitabine (%)	Prodrug (%)
Gemcitabine	50	50	
5′-L-Phenylalanyl- gemcitabine	0	18	82
5′-D-Phenylalanyl- gemcitabine	0	31	69
5′-L-Valyl-gemcitabine	0	15	85
5′-D-Valyl-gemcitabine	0	10	90

Table 4

Composition of gemcitabine and gemcitabine prodrugs (100 μM) in AsPC-1 cell uptake studies (mean ± SD, *n* = 3).

Compound	Cytosine (%)	Gemcitabine (%)	Prodrug (%)
Gemcitabine	10	90	
5′-L-Phenylalanyl- gemcitabine	10	84	6
5′-D-Phenylalanyl- gemcitabine	1	87	12
5′-L-Valyl-gemcitabine	20	11	69
5′-D-Valyl-gemcitabine	4	77	19

Table 5

Apparent (P_{app}) and effective (P_{eff}) permeability coefficients of gemcitabine and its amino acid ester prodrugs in the apical-to-basolateral direction across Caco-2 monolayer and *in situ* perfusion study in mouse (mean ± SD, $n = 3$).

Prodrug/drug	P_{app}, Caco-2 ($\times 10^{-6}$ cm/s)	P_{eff}, mouse perfusion ($\times 10^{-5}$ cm/s)
Gemcitabine	1.0 ± 0.2	2.0 ± 0.2
5′-L-Phenylalanyl-gemcitabine	3.8 ± 0.9*	33.8 ± 3.4*
5′-D-Phenylalanyl-gemcitabine	4.5 ± 0.9*	21.6 ± 4.1*
5′-L-Valyl-gemcitabine	4.0 ± 0.1*	35.8 ± 9.2*
5′-D-Valyl-gemcitabine	3.9 ± 0.1*	19.1 ± 6.1*

* $p < 0.05$, Compared with gemcitabine.

Table 6

Cell growth inhibition in AsPC-1 cells (mean ± SD, n = 3–6).

Prodrug/drug	GI_{50} AsPC-1 (mM)
Gemcitabine	10.2 ± 1.6
5′-L-Phenylalanyl-gemcitabine	4.3 ± 1.5*
5′-D-Phenylalanyl-gemcitabine	5.6 ± 1.1*
5′-L-Valyl-gemcitabine	2.0 ± 0.8*
5′-D-Valyl-gemcitabine	2.2 ± 0.9*

* $p < 0.05$, Compared with gemcitabine.